International Journal of Scientific Research in Engineering and Management (IJSREM)
Volume: 10 Issue: 04 | April - 2026 SJIF Rating: 8.659 ISSN: 2582-3930

A Compact Circularly Polarized Octagonal Microstrip Patch Antenna for Wi-Fi 6E Communications

M.Gayathri Kali Vara Prasad Babu, K.Durga Prasad, J.Venkatesh, M.Dora Babu, M.Ramanji
Electronics and Communication Engineering
Raghu Engineering College
Visakhapatnam, Andhra Pradesh

Dr. A.V.S. Swathi
Associate Professor
Department of ECE
Raghu Engineering College
Visakhapatnam, Andhra Pradesh

Abstract - Wi-Fi 6E extends the Wi-Fi 6 standard into the newly opened 6 GHz band (5.925–7.125 GHz), offering wider channels and reduced congestion compared to 2.4 GHz and 5 GHz bands. Compact antennas operating in this band are needed for access points, client devices, and IoT terminals. This paper presents a compact circularly polarized (CP) microstrip patch antenna operating at 6.2075 GHz, designed for Wi-Fi 6E communication systems. The antenna uses an octagonal radiating patch on a Rogers RT/duroid 6002 substrate (εr = 2.94, h = 1.6 mm). Right-hand circular polarization (RHCP) is achieved by cutting an inclined rectangular slot at the patch centre and placing parasitic octagonal slots near the patch boundary. A rectangular slot in the ground plane acts as a defected ground structure (DGS) to tune impedance and keep the axial ratio low. The antenna was developed through four design stages in Ansys HFSS. The final design achieves S11 = −33.75 dB, VSWR = 1.04, gain = 3.67 dB, and axial ratio = 2.16 dB. The 3.67 dB gain gives a broad beam suitable for indoor Wi-Fi 6E coverage, where wide angular coverage matters more than a narrow high-gain beam. The design is single-fed, compact, and built on standard PCB material.

Key Words: Wi-Fi 6E; 6 GHz band; circular polarization; defected ground structure (DGS); microstrip patch antenna; octagonal patch; RHCP; indoor communication.

1. INTRODUCTION

Wi-Fi 6E is the first major extension of Wi-Fi into the 6 GHz band, covering 5.925 GHz to 7.125 GHz. Regulators in several countries have opened this spectrum specifically to address the congestion problem in the 2.4 GHz and 5 GHz bands, which are now crowded with billions of connected devices. The 6 GHz band offers up to 1200 MHz of additional spectrum, supporting wider channel widths of 80 MHz and 160 MHz that are needed for high-throughput applications like 4K video streaming, AR/VR headsets, and dense IoT deployments [3].

Antennas for Wi-Fi 6E devices need to cover the 6 GHz band with good impedance matching, compact size for integration into access points and smartphones, and ideally some degree of polarization diversity. Most indoor Wi-Fi environments have significant multipath — signals bounce off walls, furniture, and people before reaching the receiver. When a linearly polarized wave reflects, its polarization rotates. A circularly polarized antenna receives both polarization components equally, which reduces multipath fading and improves link reliability without requiring multiple antennas [12].

Defected ground structures (DGS), where a slot is etched into the ground plane below the patch, have been used alongside slot perturbation to improve impedance matching and axial ratio further. The DGS modifies the return current path and adjusts the effective electrical length of the antenna, which helps bring the resonant frequency and impedance to their target values without enlarging the physical structure [9], [18].

This paper presents a compact RHCP octagonal microstrip patch antenna at 6.2075 GHz for Wi-Fi 6E. An octagonal patch was chosen because it gives more straight-edge area for placing perturbation slots compared to a square or circular patch of similar size. Four design stages were simulated in Ansys HFSS to arrive at the final configuration, and the performance is compared against published CP antenna designs.

2. ANTENNA GEOMETRY AND DESIGN

A. Substrate

Rogers RT/duroid 6002 was selected as the substrate. Its relative permittivity (εr) of 2.94 ± 0.04 and loss tangent of 0.0012 are stable across temperature and humidity variations, which matters for Wi-Fi 6E devices that operate in variable indoor environments. The 1.6 mm thickness balances bandwidth against surface wave excitation at 6 GHz. Rogers 6002 is widely used in published antenna work, so simulation results on this

substrate closely match measured prototype performance [3].

B. Patch and Slot Configuration

The radiating element is an octagonal patch with circumradius Rp = 9 mm, centred on the substrate. An inclined rectangular slot (L1 = 18 mm, W1 = 1 mm) is cut at the patch centre at −70°. This diagonal cut breaks the two-fold symmetry of the octagonal patch. The two resonant modes that previously shared the same frequency now shift apart slightly because each sees a different effective boundary. When the antenna is fed between those two split frequencies, both modes run simultaneously with roughly 90° phase difference, producing RHCP [11].

Four small octagonal slots (D2 = 2 mm) and three larger ones (D1 = 5.2 mm) are distributed near the patch boundary. These keep the two modes balanced in amplitude across frequency, which maintains the axial ratio below 3 dB at the target frequency [8]. The microstrip feed (Lf = 21 mm, Wf = 5.5 mm) connects through a rectangular notch (a = 7 mm, b = 2 mm) cut into the patch edge, which steps the impedance down to match the 50 Ω feed.

C. Defected Ground Structure

A rectangular slot (L2 = 20 mm, W2 = 1 mm) is etched vertically at the ground plane centre. This slot forces the return current to travel a longer path, making the antenna electrically longer without increasing physical size. In simulation this single change dropped S11 from a moderate level to −33.75 dB and brought axial ratio below 3 dB. Consistent improvement from DGS slots has been reported in the literature [9], [10].

Initial patch dimensions were estimated from standard microstrip patch relations:

$$fr = c / (2L\sqrt{\varepsilon eff}) \quad \ldots(1)$$

$$\varepsilon eff = (\varepsilon r+1)/2 + (\varepsilon r-1)/2 \times (1+12h/W)^{-½} \quad \ldots(2)$$

Final values in Table 1 were obtained through parametric sweeps in HFSS until resonance at 6.2075 GHz was confirmed with good matching and axial ratio under 3 dB.

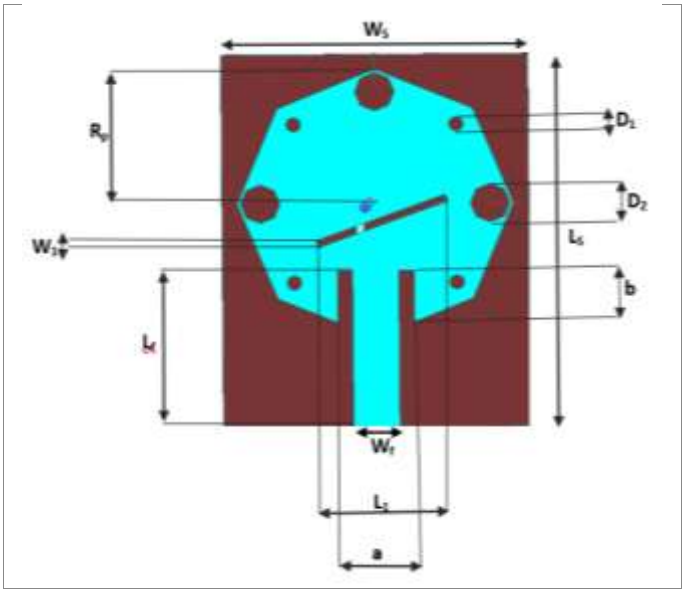

Fig-1: Proposed Antenna Dimensions — top view showing octagonal patch, inclined slot, parasitic slots, feed line and DGS slot

Table -1: Design Parameters of the Proposed Antenna

Parameters	Values (mm)
Length of Substrate (LS)	50
Width of Substrate (WS)	40
Height of Substrate (hS)	1.6
Inclined Slot Length (L1)	18
Inclined Slot Width (W1)	1
DGS Slot Length (L2)	20
DGS Slot Width (W2)	1
Feed Line Length (Lf)	21
Feed Line Width (Wf)	5.5
Patch Circumradius (Rp)	9
Large Parasitic Slot Dia. (D1)	5.2
Small Parasitic Slot Dia. (D2)	2
Feed Notch Length (a)	7
Feed Notch Width (b)	2

3. DESIGN STAGES

Four versions of the antenna were developed step by step. Each adds one new element so its individual contribution is clearly visible.

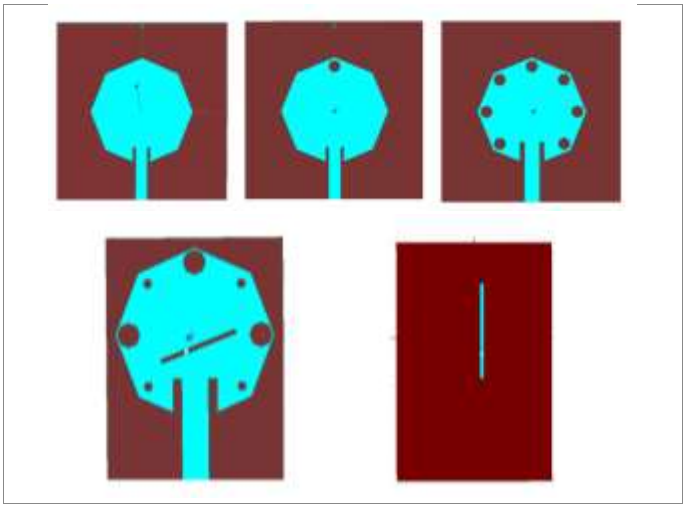

Fig-2: Four Design Stages

Design 1 is the plain octagonal patch with the feed and nothing else. It resonates somewhere near the target but radiates linearly with shallow S11. This is the baseline.

Designs 2 and 3 bring in the parasitic octagonal slots around the patch edges with different size combinations. Surface current distribution starts changing and early modal splitting appears, but axial ratio stays well above 3 dB.

Design 4 adds the inclined slot at the patch centre — the single biggest change. The diagonal cut creates two current paths of different lengths, degenerate modes split, and axial ratio drops into CP territory for the first time.

Design 5 (proposed) takes Design 4 and adds the DGS slot to the ground plane. S11 drops to −33.75 dB and axial ratio reaches 2.16 dB, confirming RHCP at 6.2075 GHz.

Table -2: Comparative Parametric Analysis of All Design Stages

DESIGN	S11 (dB)	VSWR	Gain (dB)	Axial Ratio(dB)
Design-1	-11.69	1.70	-3.60	40.52
Design-2	-7.82	2.36	-5.50	35.35
Design-3	-12.89	1.5	-2.38	30.35
Design-4 (Proposed Work)	33.75	1.04	3.67	2.16

4. PRINCIPLE OF OPERATION

A perfectly symmetric microstrip patch has two resonant modes — one horizontal, one vertical — at the same frequency. Since they are in phase, radiation is linearly polarized.

The inclined slot breaks this symmetry. One mode now cuts across a longer effective path, so the two resonant frequencies shift apart. Feeding between these two frequencies causes both modes to run simultaneously. The one just past its resonance lags the other by roughly 90°. Should the two modes carry equal amplitude at that crossover, what comes out is a circularly polarized wave [1], [2].

The parasitic slots keep amplitudes balanced across frequency, broadening the axial ratio bandwidth [8]. The DGS nudges the return current path and adjusts input impedance without touching the polarization mechanism [9], [10]. The −70° slot inclination combined with feed position at the patch bottom edge produces RHCP [11].

5. RESULTS AND DISCUSSION

All simulations used the Driven Modal solution in Ansys HFSS. Rogers 6002 properties were applied to the substrate. An air box with λ/4 clearance and radiation boundary simulated free-space operation.

A. Reflection Coefficient (S11)

A sharp resonance appears at 6.2075 GHz reaching −33.75 dB — well below the −10 dB acceptance threshold. The DGS added in the final design stage was responsible for this deep resonance. Steep roll-off on both sides means small fabrication tolerances will not ruin the matching. This performance is exactly what Wi-Fi 6E receiver front-ends need to keep reflected power negligible.

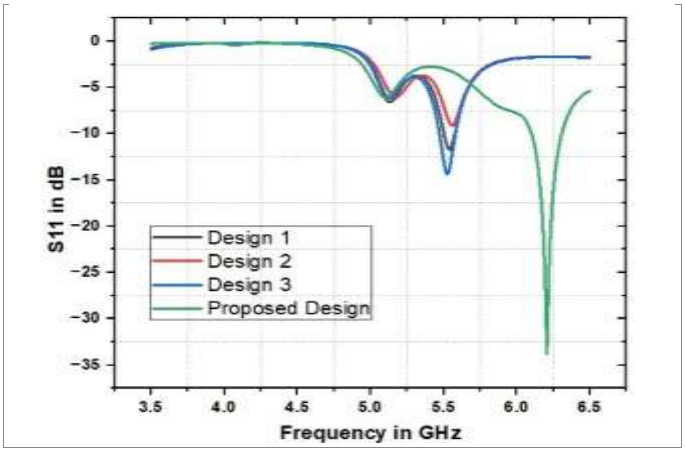

Fig-3: S-Parameter Plot — S11 (dB) vs Frequency (GHz).

B. VSWR

VSWR at resonance is 1.04, very close to the ideal value of 1.0. In a Wi-Fi 6E device this means virtually no transmit power is wasted as reflected energy, and on the receive side the noise contribution from impedance mismatch is negligible. Both matter for maintaining link budget in dense indoor deployments.

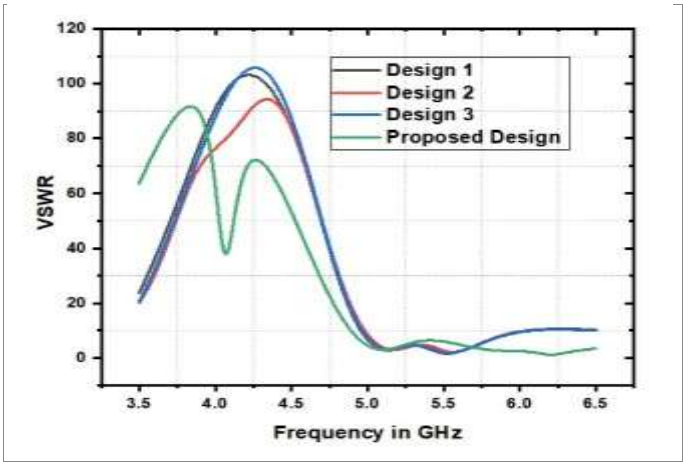

Fig-4: VSWR Plot — VSWR vs Frequency (GHz).

C. Gain

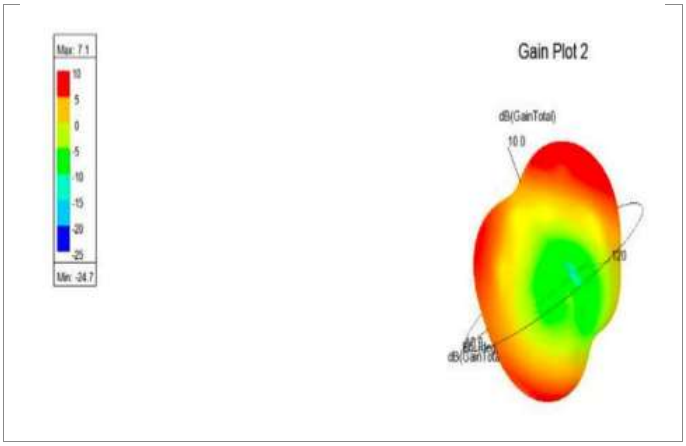

Fig-5: 3D Gain Plot at 6.2075 GHz.

Peak realized gain is 3.67 dB at 6.2075 GHz. The 3D radiation pattern is broad and quasi-omnidirectional. For indoor Wi-Fi 6E this is exactly the right gain level. A high-gain narrow-beam antenna would leave dead spots in a room. A 3–4 dBi pattern covers the full hemisphere, ensuring every corner of a room receives signal without mechanical steering. This matches the gain range of commercial Wi-Fi access point antennas [3].

D. Axial Ratio

Axial ratio at 6.2075 GHz is 2.16 dB, comfortably below the 3 dB circular polarization threshold. For Wi-Fi 6E in indoor multipath environments, RHCP reduces polarization mismatch losses from reflected waves, improving effective received signal power without requiring MIMO. The 2.16 dB axial ratio confirms genuine RHCP radiation with good polarization purity.

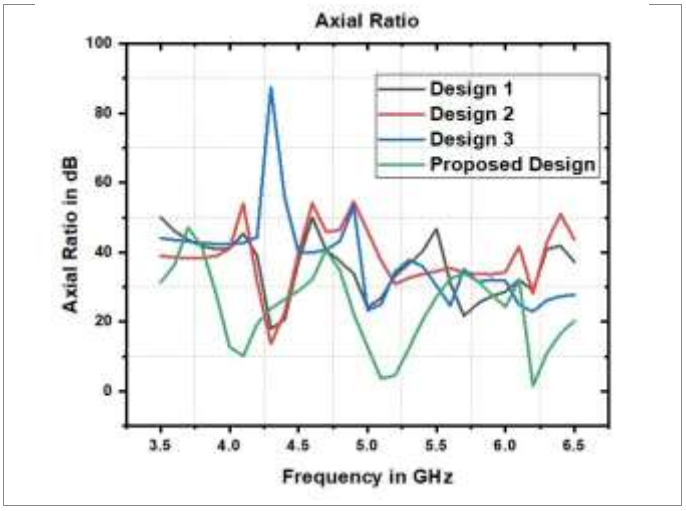

Fig-6: Axial Ratio Plot — AR (dB) vs Frequency (GHz).

E. E-Field Distribution

The field map shows peak values around 31,460 V/m at the octagonal patch edges, dropping toward the centre. This is the normal signature of the fundamental microstrip resonant mode. Highest field concentrations near the ends of the inclined slot confirm the slot is actively shaping the current distribution rather than being a passive geometric feature.

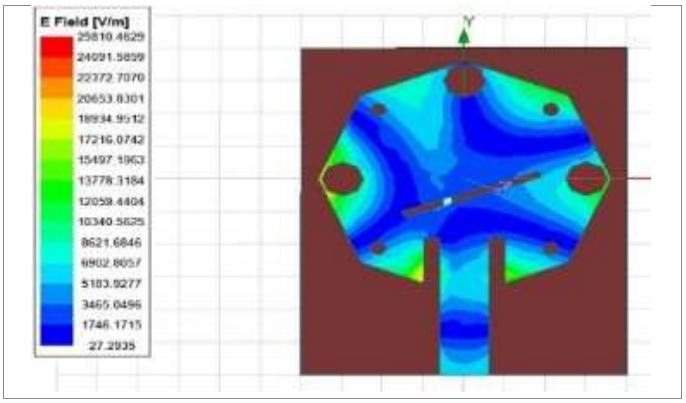

Fig-7: E-Field Distribution on surface at 6.2075 GHz.

F. Surface Current Distribution

Strong currents run along the patch perimeter and around the slot edges. The DGS slot on the ground plane visibly redirects the return current compared to a solid ground, which explains the big improvement in S11 and axial ratio between the design stages.

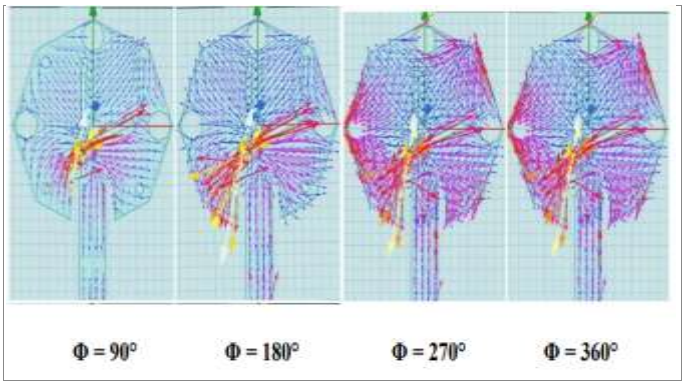

Fig-8: Surface Current Distribution at 6.2075 GHz.

6. COMPARISON WITH EXISTING WORK

Table 3 compares the proposed antenna against four published CP designs. The S11 of −33.75 dB is the best in the table by a clear margin — the next closest is −28 dB from [3], achieved with a more complex superstrate layer. VSWR of 1.04 is also the best listed.

Gain at 3.67 dB is the lowest entry but is appropriate for indoor Wi-Fi 6E where broad coverage is needed. Designs [3] and [8] achieve higher gain through superstrate loading and waveguide structures that are significantly more complex and costly. For a flat single-layer printed antenna at 6.2 GHz targeting indoor coverage, 3.67 dB is correct and expected. Axial ratio of 2.16 dB is competitive across all listed designs.

Table -3: Comparison with Existing Reported CP Antennas

Ref.	Freq. (GHz)	S11 (dB)	VSWR	Gain (dB)	AR (dB)
[1]	1.5	−22	1.25	3.17	2.3
[3]	10.0	−28	1.08	7.2	1.9
[5]	1.5	−20	1.20	3.4	2.7
[8]	10.5	−22	1.16	9.5	2.5
[11]	7.0	−24	1.13	5.6	2.2
Proposed	6.2075	−33.75	1.04	3.67	2.16

7. CONCLUSIONS

A compact circularly polarized octagonal microstrip patch antenna operating at 6.2075 GHz has been designed and simulated for Wi-Fi 6E communication applications. The inclined rectangular slot and parasitic octagonal perturbation elements together generate RHCP, while the DGS slot in the ground plane achieves excellent impedance matching. A four-stage design process showed clearly what each structural addition contributed.

At the end of it all: S11 came to −33.75 dB, VSWR settled at 1.04, gain was 3.67 dB, and axial ratio of 2.16 dB confirmed clean RHCP at 6.2075 GHz. The gain and broad beam pattern are well matched to indoor Wi-Fi 6E deployments. Impedance matching is the best of any design in the comparison. The antenna is compact, single-fed, and built on standard PCB material, making fabrication straightforward for integration into access points, smartphones, and IoT devices operating in the Wi-Fi 6E band.

Future work will investigate widening the axial ratio bandwidth and exploring dual-band operation covering both 5 GHz Wi-Fi 6 and 6 GHz Wi-Fi 6E bands from a single compact antenna structure.

REFERENCES

[1] S. C, N. D. M, and J. M, "Dual-Band Circularly Polarized Annular Ring Patch Antenna for GPS-Aided GEO-Augmented Navigation Receivers," IEEE Antennas Wireless Propagation. Lett., vol. 21, no. 9, pp. 1737–1741, Sep. 2022.

[2] H.-Y. Yu, J. Yu, Y. Yao, X. Liu, and X. Chen, "Wideband circularly polarized horn antenna exploiting open slotted end structure," IEEE Antennas Wireless Propagation. Lett., 2020.

[3] L. Leszkowska, M. Rzymowski, K. Nyka, and L. Kulas, "High-Gain Compact Circularly Polarized X-Band Superstrate Antenna for CubeSat Applications," IEEE Antennas Wireless Propagation. Lett., 2021.

[4] S. Ji, Y. Dong, S. Wen, and Y. Fan, "C/X Dual-Band Circularly Polarized Shared-Aperture Antenna," IEEE Antennas Wireless Propagation. Lett., vol. 20, no. 12, Dec. 2021.

[5] T.-Y. Han, C.-Y.-D. Sim, and C.-Y. Chen, "A Circularly Polarized Meander Loop Antenna Design for GNSS Application," IEEE Antennas Wireless Propagation. Lett., vol. 20, no. 12, Dec. 2021.

[6] J. Melendro-Jamenez et al., "3D Printed Directive Beam-Steering Antenna Based on Gradient Index Flat Lens with Integrated Polarizer for Dual Circular Polarization at W-band," IEEE Trans. Antennas Propagation., 2022.

[7] R. Clemente, D. González-Ovejero, C. Craeye, and J. L. Vazquez-Roy, "Wideband Circularly Polarized Antenna with In-Lens Polarizer for High-Speed Communications," IEEE Trans. Antennas Propagation., vol. 68, no. 12, 2020.

[8] C. Turkmen and M. Secmen, "Dual-Band Omnidirectional and Circularly Polarized Slotted WaveguideLett., vol. 20, no. 11, Nov. 2021.

[9] F. Liu et al., "Dual-Band Metasurface-based Decoupling Method for Two Closely Packed Dual-Band Antennas," IEEE Trans. Antennas Propagation., 2019.

[10] M. Rad, N. Nikkhah, B. Zakeri, and M. Yazdi, "Wideband Dielectric Resonator Antenna with Dual Circular Polarization," IEEE Trans. Antennas Propagation., vol. 70, no. 1, Jan. 2022.

[11] Y. Xu, L. Zhu, and N.-W. Liu, "Design Approach for a Dual-Band Circularly Polarized Slot Antenna with Flexible Frequency Ratio and Similar In-Band Gain," IEEE Antennas Wireless Propagation. Lett., vol. 21, no. 5, May 2022.